Iron porphyrin attached to single-walled carbon nanotubes: Electronic and dynamical properties from *ab initio* calculations

Igor Ruiz-Tagle and Walter Orellana
Departamento de Ciencias Físicas, Universidad Andres Bello, Av. República 220, 837-0134 Santiago, Chile
(Received 27 May 2010; revised manuscript received 11 July 2010; published 7 September 2010)

Covalent and noncovalent attachment of an iron porphyrin (FeP) on the surface of single-walled carbon nanotubes (CNTs) are addressed by density-functional-theory calculations and molecular-dynamic simulations. We investigate the stability and electronic properties of several CNT-FeP assemblies in order to shed light in the experimentally reported electrocatalytic activity of carbon-supported Fe macrocycles and the role of the linking structure. Two mechanisms for the FeP attachment on metallic and semiconducting CNTs were considered: by physisorption through π-π stacking interaction and by chemisorption through sp^2 and sp^3 bonding configurations. Our results suggest that FeP covalently linked to metallic CNTs would be the best electrocatalytic systems due to its metallic character at room temperature, suggesting that they may work as an electrode with the ability to transport charge to the macrocycle. Semiconducting CNTs would be unlikely because the FeP-CNT assembly preserves the semiconducting character. Noncovalent attachment of FeP onto both CNTs is also unlikely due to the absence of physical contact and the unsuccessful FeP fixation.

DOI: 10.1103/PhysRevB.82.115406 PACS number(s): 73.22.−f, 68.43.Bc, 68.43.Hn

I. INTRODUCTION

The search for nonprecious metal catalysts that can substitute platinum in polymer electrolyte membrane fuel cells (PEMFCs) for the oxygen-reduction reaction (ORR) is one of the key problems to be solved for the massive use of hydrogen as fuel in transportation. Efforts to replace this scarce and expensive metal by alternative low-cost and abundant catalysts with similar chemical stability and catalytic activity toward the ORR are still fruitless.

Transition metal-N_4 macrocycles such as phthalocyanine and porphyrin have been widely investigated as catalysts for ORR since the seminal work of Jasinski who observed that cobalt phthalocyanine can catalyze this reaction in an alkaline solution.[1] Later experiments showed that carbon-supported Fe-N_4 and Co-N_4 macrocycles can also catalyze ORR in an acidic medium[2] but a rapid decline in the catalytic activity was observed. However, an important advance was the discovery that heat treatments of carbon supported metal-N_4 macrocycles in a range from 600 °C to 1000 °C improves the stability and activity for the ORR catalysis.[3,4]

Recently, the same iron-macrocycles atomic structure (Fe-N_4) supported on microporous carbon have shown ORR activity comparable to those observed on Pt-based catalysts.[5] Others configurations of the same elements, namely, (Fe,Co)/N/C, formed after pyrolysis at high temperature have shown catalytic activity for ORR in PEMFC cathode.[6] In addition, Co porphyrin anchored to multiwalled carbon nanotubes (CNTs) have shown superior catalytic performance for ORR in acidic medium at room temperature, demonstrating the advantages of supramolecular complex formed by electrocatalytic metallomacrocycles covalently linked to CNTs.[7] However, the nature of the active sites and the origin of the improved catalytic activity of these systems is still unknown. Theoretical works in the subject are limited to investigate the noncovalent adsorption of porphyrins and metalloporphyrins on CNT sidewalls.[8,9] In these articles is suggested a stronger chemical reactivity for macrocycles physisorbed on semiconducting than on metallic CNTs, which would be effective to separate them.

In this work we investigate the stability and electronic properties of an iron porphyrin (FeP) covalently and noncovalently linked to metallic and semiconducting single-walled CNTs using *ab initio* calculations. Three different geometries for the FeP-CNT assembly were considered to emulate plausible configurations that could be formed after heat treatment. Catalytic properties of the FeP-CNT assemblies are analyzed in term of their electronic band structure.

II. THEORETICAL APPROACH

Our density-functional-theory (DFT) calculations were performed using the SIESTA *ab initio* package,[10] which employs norm-conserving pseudopotentials and localized atomic orbitals as basis set (double-ζ plus polarization functions in the present work). Two different mechanisms for the macrocycle attachment on the CNT sidewalls are considered: by physisorption through π-π stacking interaction and by chemisorption through sp^2 and sp^3 bonding configurations. The FeP physisorption is investigated by Van der Waals density functional as proposed by Dion *et al.*[11] and recently implemented in the SIESTA code.[12] Whereas, the FeP chemisorption is investigated by standard DFT using the local-density approximation (LDA) to the exchange-correlation functional.[13] We used LDA because gave us better results for carbon structures than the generalized gradient approximation (GGA).[14] For diamond, the LDA (GGA) band gap is calculated to be 4.17 eV (4.14 eV), which is about 24% smaller that the experimental value. Whereas, the LDA (GGA) lattice parameter is found to be of 3.562 Å (3.597 Å), which is −0.1% (+0.8%) of the experimental value.

Two single-walled CNTs with 11 Å in diameter were chosen as the FeP supports: The metallic (8,8) and the semiconducting (14,0), the latter with a LDA band gap of 0.73 eV. We consider supercells with periodic boundary condi-

TABLE I. Relative energy (ΔE) and average bond lengths (d) of the isolated iron porphyrin (FeP) in different spin multiplicities. Energy and distances are in eV and Å, respectively.

	LDA			GGA		
Parameter	^{1}FeP	^{3}FeP	^{5}FeP	^{1}FeP	^{3}FeP	^{5}FeP
ΔE	0.66	0.0	1.17	0.61	0.0	0.61
d(Fe-N)	1.94	1.95	2.01	1.99	1.99	2.06
d(N-C)	1.39	1.40	1.38	1.40	1.40	1.39

tions along the nanotube axis, containing up to 7 CNT unit cells. The lateral separation between CNT images is chosen to be of 10 Å. Due to the large supercell size, the Brillouin zone sampling was performed with the Γ point. Tests of convergence for the band structure of metallic systems were performed considering up to 12 **k** points. The results indicate that our single **k**-point calculations are converged. The FeP-CNT binding energy is calculated by the energy difference between adsorbed and separated constituents, considering corrections due to the basis set superposition error. The systems were fully relaxed until all force components were smaller than 0.05 eV/Å. The room-temperature structural behavior of FeP attached to the CNTs are investigated by constant-temperature *ab initio* molecular dynamic, using the Nosé-thermostat approach.[15] In this formalism, the system is in thermal contact with a heat bath, which can exchange energy in order to fix the system temperature, simulating a canonical ensemble. Molecular-dynamic (MD) simulations are performed over a time of 1 ps with a time step of 1 fs. The equilibrium geometries of all CNT-FeP systems at 0 K were obtained by additional thermal annealing during 0.5 ps.

Table I shows results for equilibrium geometry and relative energy of an isolated FeP in different spin multiplicities. Here we include GGA results for comparison. Both LDA and GGA calculations show a triplet ground state whereas the singlet state is found to be about 0.6 eV higher in energy. However, in the quintet state LDA and GGA calculations shows a large energy difference, of about 0.6 eV. This difference can be associated with the overestimation of the bond strength by LDA which tends to increase the energy for the high-spin state (^{5}FeP) as a consequence of populating an antibonding molecular orbital.[16] Our GGA results are in good agreement with previous calculations for the isolated FeP of Ref. 16. In the present work only the FeP ground-state spin multiplicity will be considered.

The interaction mediating metalloporphyrins adsorption on CNT sidewalls is believed to be noncovalent. Experiments have explored the immobilization of such macrocycles onto graphite and CNTs showing a strong mutually interacting π systems with charge transfer features.[17,18] From the theoretical point of view, a recent DFT calculation explores the adsorption of metalloporphyrins on the CNT sidewall using GGA to the exchange-correlation potential.[9] Here, it is suggested a separation mechanism between metallic and semiconducting CNTs interacting with metalloporphyrins, which is attributed to a difference in charge transfer and hybridization. However, DFT-GGA calculations are known to fail for cases where the adsorption is dominated by Van der Waals interactions. Therefore, we believe that this study cannot be considered conclusive.

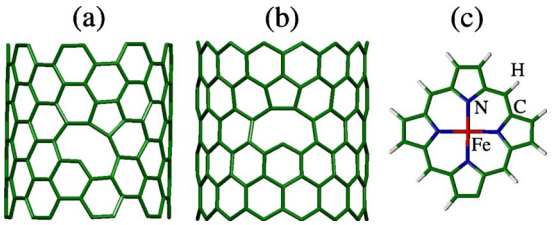

FIG. 1. (Color online) Equilibrium geometries of CNTs with a single vacancy: (a) (8,8)+V and (b) (14,0)+V. (c) The FeP radical with a missing H atom (FeP*).

The FeP chemisorption on the pristine CNTs were induced by removing a H atom from FeP in order to allow the formation of a sp^3-like C-C bond between the CNT and the FeP radical (hereafter FeP*). In addition, the single vacancy in CNTs offers an alternative mechanisms to anchored the FeP* by a sp^2-like C-C bond. Previous DFT calculations have shown that a single vacancy in (8,8) and (14,0) CNTs [hereafter (8,8)+V and (14,0)+V], spontaneously reconstructs leaving a twofold coordinated C atom with an unpaired electron.[19] Fig. 1 shows the equilibrium geometries of the single vacancy in (8,8) and (14,0) CNTs as well as the FeP* geometry. Vacancy defects in CNTs are currently induced by irradiation with energetic electrons.[20] Thus, we propose that twofold coordinated C atoms in CNTs, as created by vacancy defects, can be used as active sites for the covalent attachment of FeP*.

III. RESULTS AND DISCUSSION

A. FeP-CNT structural properties

Figure 2 shows our results for the equilibrium geometries of FeP attached on the pristine (8,8) CNT by physisorption

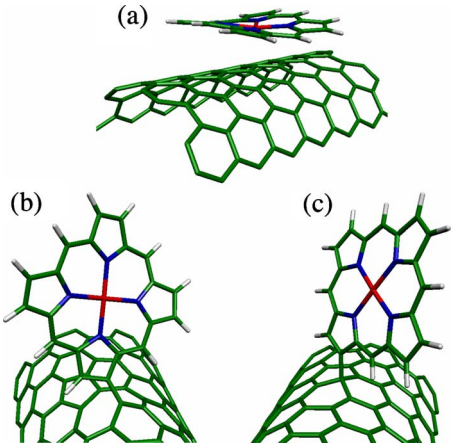

FIG. 2. (Color online) Equilibrium geometries of FeP and FeP* adsorbed on the metallic (8,8) CNT. (a) FeP physisorption on the perfect CNT. (b) FeP* chemisorption on the defective (8,8)+V CNT by sp^2 bonding. (c) FeP* chemisorption on the perfect CNT by sp^3 bonding.

[Fig. 2(a)], and FeP* attached on both pristine (8,8) and defective (8,8)+V CNTs by chemisorption [Figs. 2(b) and 2(c), respectively]. For the physisorption, the FeP equilibrium geometry is found at 3.13 Å from the CNT surface where the Fe atom of the macrocycle projects onto the center of a C-C bond of the CNT. Total charge density plots (not shown) indicated that no chemical bond between FeP and the CNT are formed, which confirm a Van der Waals-type interaction between the macrocycle and the π-electronic surface of CNT. We find a rather large FeP binding energy of −1.09 eV, suggesting an unusually strong π-π stacking interaction which agrees with experimental reports in related systems.[17,18] For the FeP physisorption on the (14,0) CNT a similar result is found. The FeP binding energy is calculated in −1.05 eV while the macrocycle locates at 3.16 Å from the CNT surface. Thus we find that the FeP interaction with metallic or semiconducting CNTs would not give signs of any selectivity. This result agrees with experiments that show a selective interaction between metal-free porphyrins and semiconducting CNTs but not with metalloporphyrins.[21]

For the sp^2 chemisorption on the metallic CNT [FeP*-(8,8)+V], a strong C-C bond of 1.42 Å in length links the FeP* to the twofold coordinated C atom of (8,8)+V with a binding energy of −5.0 eV. Here, the FeP* plane forms an angle of about 65° with the CNT surface [Fig. 2(b)]. This equilibrium position can be understood as a compensation of forces between the elastic force that tends to put together the macrocycle on the CNT wall and the FeP-CNT steric force. The sp^2 chemisorption on the semiconducting CNT [FeP*-(14,0)+V] shows slightly different results. The FeP* binding energy is calculated in −4.8 eV, where the linking C-C bond is find to be of 1.40 Å. Here, the FeP* plane forms an angle of about 80° with the CNT surface. Different geometries of FeP* in the sp^2 configuration can be understood by inspecting the different vacancy structure in the (8,8) and (14,0) CNTs, as shown Figs. 1(a) and 1(b), respectively.

For the sp^3 chemisorption on the metallic CNT [FeP*-(8,8)], a weaker C-C bond of 1.53 Å links the FeP* to the pristine (8,8) CNT with a binding energy of −1.6 eV. In the equilibrium geometry, the CNT atom of this C-C bond protrudes out the nanotube surface by about 0.4 Å, forming a diamondlike sp^3 hybridization. While FeP* stands normal to the CNT surface and diagonal to the CNT axis to minimize the FeP-CNT steric repulsion, which also tend to twist the macrocycle [Fig. 2(c)]. The sp^3 chemisorption on the semiconducting CNT [FeP*-(14,0)] shows similar results, a C-C bond of 1.53 Å links the FeP* to the pristine (14,0) CNT with a binding energy of −1.8 eV. Room-temperature MD simulations show that chemisorbed FeP* on both CNTs swings and twists around the sp^2 and sp^3 anchoring positions. While for the physisorption, FeP moves onto the CNT surfaces without desorption. Hence, the potential energy surfaces of the FeP-CNT systems after 1 ps are rather simple and, due to the relatively low-temperature, dissociative reactions are not expected. Therefore, we believe that the FeP-CNT structural behavior at room temperature should not change for longer simulation times.

The above results show that the sp^2 attachment is the strongest way to anchor a FeP* on a CNT, but it needs a vacancy defect with a twofold coordinated atom that cost about 5 eV to be created, as shown formation energy calculations of Ref. 19. However, in the weaker sp^3 attachment, FeP* can be directly linked to the pristine CNT, suggesting a straightforward mechanism to anchor macrocycles on CNT sidewalls. Follow this idea, we investigate the formation of the sp^3 attachment by MD simulation at high temperatures, starting from the equilibrium geometry of FeP physisorbed on the pristine (8,8) CNT. Our results show that about 1000 °C, the H atoms becomes to desorb from FeP while the CNT preserves its structure, indicating that heat treatments could be an effective way to covalently link macrocycles on CNTs. Interestingly, recent experiments have reported similar procedure to synthesized catalysts formed by Co and Fe macrocycles supported on CNTs, which have shown higher ORR activity than the same macrocycles supported on graphite or commercial Pt/C catalysts.[22] These findings suggest a central role for the covalent attachment and the use of CNTs as an electrode material in electrochemical reactions.

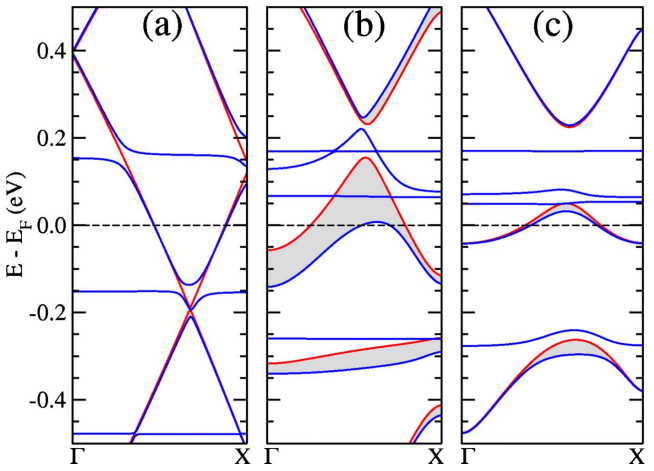

FIG. 3. (Color online) Spin-resolved band structure of FeP adsorbed on the metallic (8,8) CNT. (a) π-π stacking, (b) sp^2 bonding, and (c) sp^3 bonding. Blue (red) lines indicate majority (minority) spin subbands and shaded areas the exchange splitting.

B. FeP-CNT electronic properties

Figure 3 shows the spin-resolved band structure of FeP attached on the metallic (8,8) CNT by physisorption [Fig. 3(a)], and sp^2 and sp^3 chemisorptions [Figs. 3(b) and 3(c), respectively]. First we note that the metallic character of the (8,8) CNT is preserved after the FeP adsorption in all configurations. However, as the physisorbed FeP has the obvious charge transfer limitation with the CNT, due to the absence of physical contact, this kind of adsorption would not be suitable to link macrocycles for catalysis. The physisorption band structure shows the Fe 3d orbitals at ±0.15 eV with respect to the Fermi level, perturbing the (8,8) CNT subbands at the crossing points and shifting the CNT Fermi level upward by about 0.2 eV. This suggests a rather strong Van der Waals interaction which is also reflected in the large FeP-(8,8) binding energy, of about 1 eV. This strong π-π stacking interaction can be associated with

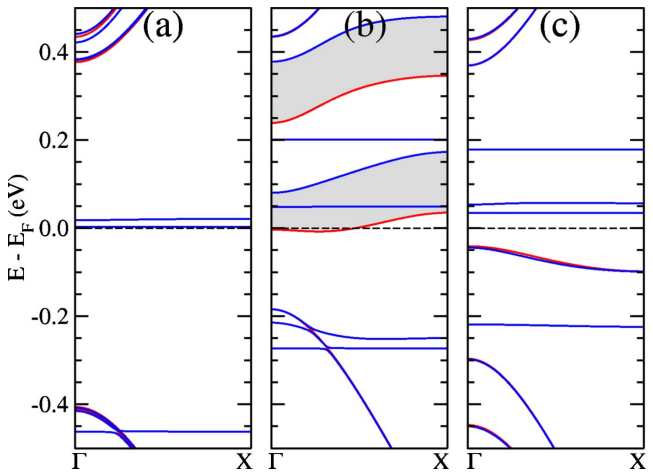

FIG. 4. (Color online) Spin-resolved band structure of FeP adsorbed on the semiconducting (14,0) CNT. (a) π-π stacking, (b) sp^2 bonding, and (c) sp^3 bonding. Blue (red) lines indicate majority (minority) spin subbands and shaded areas the exchange splitting.

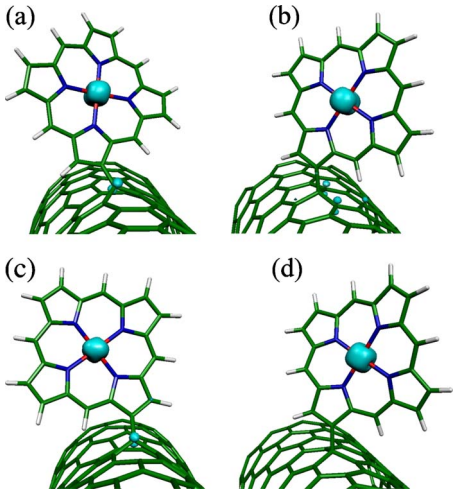

FIG. 5. (Color online) Charge density isosurfaces for the states that cross the Fermi level of the metallic systems: (a) (8,8)-FeP sp^2, (b) (8,8)-FeP sp^3, and (c) (14,0)-FeP sp^2. (d) Charge density for the states at top of the valence band of the semiconducting system (14,0)-FeP sp^3. The isosurfaces correspond to a charge of 0.005 $e/\text{Å}^3$.

the large FeP-CNT contact area. In the case of FeP chemisorptions, both sp^2 and sp^3 covalent bonds give a metallic character for the FeP-CNT assembly, as shown Figs. 3(a) and 3(b), suggesting favorable conditions for metallic CNTs to work as electrodes. The band structure shows a strong hybridization between the Fe 3*d* orbitals and the (8,8) CNT bands at the Fermi level. In addition, for the sp^2 attachment we find a larger splitting between majority and minority spin subbands, of about 0.1 eV, which is not observed for sp^3 [shaded area in Figs. 3(a) and 3(b)]. This exchange splitting can be attributed to the higher FeP-CNT steric repulsion exhibits in the sp^2 geometry.

Figure 4 shows the electronic structure of FeP attached on the semiconducting (14,0) CNT by physisorption [Fig. 4(a)]. Here, two empty Fe 3*d* orbitals appear as dispersionless subbands just above the Fermi level, reducing by half the (14,0) CNT band gap. For the sp^2 attachment [Fig. 4(b)], we observe a half-metallic behavior which is originated in the exchange splitting of the sp^2 configuration as discussed above. Whereas for the sp^3 attachment [Fig. 4(c)], the system shows a semiconducting character with a LDA band gap of about 0.1 eV. According to the these results, we conclude that a semiconducting CNT changes its electronic properties after the FeP adsorption, reducing drastically its band gap in the case of π-π and sp^3 attachment and becoming metallic for sp^2.

Active sites in catalysts have the ability to exchange charge with a reactant without altering its structure, this implies that states at the Fermi level or those at the top of the valence band are key to identify active sites in the CNT-FeP systems under study. Figure 5 shows the charge density isosurfaces for the states that cross the Fermi level in the CNT-FeP metallic systems: (8,8)-FeP sp^2 and (8,8)-FeP sp^3 and (14,0)-FeP sp^2 [Figs. 5(a)–5(c), respectively]. We also include the charge density for the states at the top of the valence band in the semiconducting system (14,0)-FeP sp^3 [Fig. 5(d)]. We observe that all these relevant states originate in the Fe 3*d* orbitals, indicating that the only active site of the CNT-FeP assembly is the iron atom of FeP independently of the nature of the chemical bonds that anchor the macrocycle to the CNT. It is worthy of note that the magnetic moment of FeP is also preserved in all the FeP-CNT systems as shown in Table II, suggesting that the macrocycle spin multiplicity is not altered by the CNT support.

To verify if the electronic properties of CNT-FeP systems are maintained at room temperature we take the geometries of these systems after 1 ps of MD simulation to calculate the band structure. This procedure can give us a reasonable approach of which changes we should expect in the electronic properties of the CNT-FeP systems with temperature. Our results show that (8,8)-FeP linked by physisorption and chemisorption preserves almost unchanged their electronic properties, ensuring the ability of metallic CNTs to work as electrodes. However, for (14,0)-FeP we observe some changes in the electronic properties as shown in Fig. 6. For the physisorption [Fig. 6(a)], we find essentially the same band structure. Whereas, for the sp^2 attachment [Fig. 6(b)], the state that cross Fermi level at 0 K [Fig. 4(b)] rises with temperatures, increasing slightly the band gap. For the sp^3

TABLE II. Binding energy (E_b) and spin magnetic moment (m_s) of FeP attached on the metallic (8,8) and semiconducting (14,0) CNTs.

System	Bonding	E_b (eV)	m_s (μ_B)
FeP-(8,8)	π-π	−1.090	2.00
FeP*-(8,8)+V	sp^2	−4.997	2.20
FeP*-(8,8)	sp^3	−1.626	2.19
FeP-(14,0)	π-π	−1.051	2.06
FeP*-(14,0)+V	sp^2	−4.813	1.93
FeP*-(14,0)	sp^3	−1.796	2.16

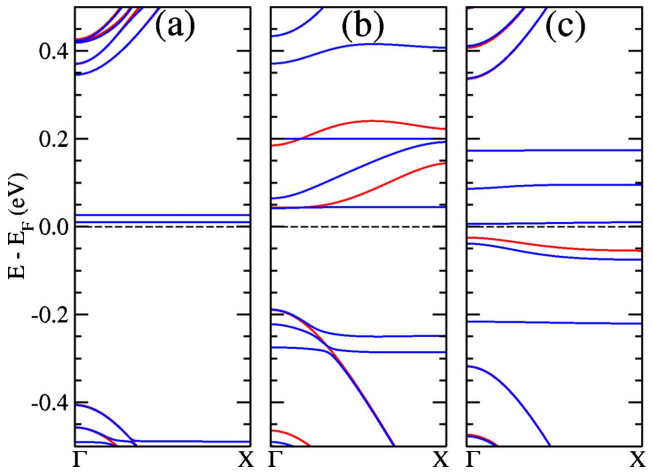

FIG. 6. (Color online) Spin-resolved band structure of FeP adsorbed on the semiconducting (14,0) CNT at 300 K. (a) π-π stacking, (b) sp^2 bonding, and (c) sp^3 bonding. Blue (red) lines indicate majority (minority) spin subbands.

chemisorption [Fig. 6(c)], we observe small variations in the band gap as compared to the 0 K band structure [Fig. 4(c)]. Therefore, the FeP-CNT semiconducting systems would preserve their electronic character at room temperature, suggesting that semiconducting CNTs would be unlikely substrate to link macrocycles.

IV. SUMMARY AND CONCLUSION

We have shown from *ab initio* calculations that metallic CNTs would be a favorable substrate to covalently link electrocatalytic macrocycles. Two major advantages for metallic CNTs have been identified: (i) chemical stability for the macrocycle preserving the Fe-N_4 active site and (ii) metallic character for the assembly so that the CNT support can work as an electrode with the ability to transport charge to the macrocycle. Our results also suggest that the FeP anchoring on pristine or defective CNT can be induced by removing H atoms from the macrocycles at high temperatures. This kind of linkage could explain the improve catalytic performance observed in carbon-supported metallomacrocycles after heat treatment at high temperatures.[7,22] On the other hand, semiconducting CNTs would be unlikely substrates because they show a small band gap after the FeP attachment, preventing an easy charge transport to the macrocycle. Whereas for noncovalent attachments, we find a strong π-π stacking interaction with a FeP binding energy of about 1 eV, which we attributed to the large CNT-FeP contact area. In spite of this strong interaction, the macrocycle cannot be fixed on the CNT at room temperature, moving freely through the surface. Thus, this kind of attachment would be unlikely to link electrocatalytic macrocycles to CNTs due to absence of physical contact, making difficult the charge transport.

ACKNOWLEDGMENTS

This work was supported by FONDECYT Grant No. 1090489, Project Anillo Bicentenario No. ACT24/2006, UNAB Grant No. DI-06-08/R, and Project Millennium Nucleus No. P07-006-F. Igor Ruiz-Tagle acknowledges UNAB Grant No. DI-12-09/I and CONICYT Grant No. 2108064.

[1] R. Jasinski, Nature (London) **201**, 1212 (1964).
[2] H. Jahnke, M. Schönborn, and G. Zimmermann, Top. Curr. Chem. **61**, 133 (1976).
[3] V. S. Bagotzky, M. R. Tarasevich, K. A. Radyushkina, O. E. Levina, and S. I. Andrusyova, J. Power Sources **2**, 233 (1978).
[4] J. P. Dodelet, in *N4-Macrocycles Metal Complexes*, edited by J. H. Zagal, F. Bedioui, and J. P. Dodelet (Springer, New York, 2006), pp. 83–147.
[5] M. Lefèvre, E. Proietti, F. Jaouen, and J.-P. Dodelet, Science **324**, 71 (2009).
[6] F. Charreteur, F. Jaouen, and J. P. Dodelet, Electrochim. Acta **54**, 6622 (2009).
[7] W. Zhang, A. U. Shaikh, E. Y. Tsui, and T. M. Swager, Chem. Mater. **21**, 3234 (2009).
[8] J. lu, L. Lai, G. Luo, J. Zhao, R. Qin, D. Wang, L. Wang, W. N. Mei, G. Li, Z. Gao, S. Nagase, Y. Maeda, K. Akasaka, and D. Yu, Small **3**, 1566 (2007).
[9] J. Zhao and Y. Ding, J. Phys. Chem. C **112**, 11130 (2008).
[10] J. M. Soler, E. Artacho, J. D. Gale, A. García, J. Junquera, P. Ordejón, and D. Sánchez-Portal, J. Phys.: Condens. Matter **14**, 2745 (2002).
[11] M. Dion, H. Rydberg, E. Schröder, D. C. Langreth, and B. I. Lundqvist, Phys. Rev. Lett. **92**, 246401 (2004).
[12] G. Román-Pérez and J. M. Soler, Phys. Rev. Lett. **103**, 096102 (2009).
[13] J. P. Perdew and A. Zunger, Phys. Rev. B **23**, 5048 (1981).
[14] J. P. Perdew, K. Burke, and M. Ernzerhof, Phys. Rev. Lett. **77**, 3865 (1996).
[15] S. Nosé, Mol. Phys. **52**, 255 (1984).
[16] C. Rovira, K. Kune, J. Hutter, P. Ballone, and M. Parrinello, J. Phys. Chem. A **101**, 8914 (1997).
[17] N. J. Tao, Phys. Rev. Lett. **76**, 4066 (1996).
[18] G. M. A. Rahman, D. M. Guldi, S. Campidelli, and M. Prato, J. Mater. Chem. **16**, 62 (2006).
[19] W. Orellana and P. Fuentealba, Surf. Sci. **600**, 4305 (2006).
[20] A. V. Krasheninnikov and F. Banhart, Nature Mater. **6**, 723 (2007).
[21] H. Li, B. Zhou, Y. Lin, L. Gu, W. Wang, K. A. S. Fernando, S. Kumar, L. F. Allad, and Y.-P. Sun, J. Am. Chem. Soc. **126**, 1014 (2004).
[22] L. Deng, M. Zhou, C. Liu, L. Liu, C. Liu, and S. Dong, Talanta **81**, 444 (2010).